

Microstructural Lattice Simulation and Transient Rheological Behavior of a Flow-aligning Liquid Crystalline Polymer under Low Shear Rates

Hansol Cho*, Mingzhe Xu, Sang Ouk Kim, Kwang Man Kim ** and In Jae Chung†

Department of Chemical Engineering, Korea Advanced Institute of Science and Technology (KAIST),
373-1 Kusong, Yusong, Taejon 305-701, Korea
(Received 24 April 2000 • accepted 16 November 2000)

Abstract—A microstructural lattice simulation for textured liquid crystalline polymer is carried out to predict rheological behavior, especially the stress evolution after shear inception. It is based on a combination of two main concepts: (i) the director in each cell of a supramolecular lattice has an orientation described by the minimization of total energy of director map, and (ii) the torque balance of each director under shear flow and anisotropic relaxational shear moduli depends on the averaged orientation of the director map. By considering the interaction between the nearest-neighbor directors, the spatial orientational correlation is introduced and the spatial heterogeneity, i.e., a polydomain texture, is generated simultaneously. For the start-up shear flow, the overshoot and the steady value of shear stress increase and the former shifts toward a shorter time as the applied shear rate increases. Also, the calculated stress evolution is compared with the experimental result of a thermotropic liquid crystalline poly(ester-imide).

Key words : Lattice Simulation, Polydomain Structure, Thermotropic Liquid Crystalline Polymer (TLCP)

INTRODUCTION

Liquid crystalline polymers (LCP), lyotropic and/or thermotropic, with rigid mesogenic unit and flexible spacers in the main chain arouse interest academically and industrially. They show a number of unusual rheological phenomena such as long relaxation time [Wissbrun, 1980], negative first normal stress difference, damped oscillatory transient stress in the case of inception of shear flow [Guskey and Winter, 1991; Kim and Han, 1993; Winter and Wedler, 1993; Baek et al., 1994; Han and Chang, 1994]. These phenomena may be explained by applying various factors: the possibility of director tumbling/wagging in a negative first normal stress, the textured or polydomain structure by the inhomogeneity of director field and so forth. Most thermotropic liquid crystalline polymer (TLCP) very often shows thermal hysteresis [Done and Baird, 1990; Driscoll et al., 1994] in which a rheological property has two different values at a certain nematic temperature on heating and cooling. It is explained by the supercooling effect. They also show the change of a rheological property with time at a fixed temperature, because residual crystallites accelerate the formation of high-temperature crystallites [Lin and Winter, 1989]. The negative value of first normal stress difference N_1 , first reported by Kiss and Porter [1978] for lyotropic liquid crystalline polymer (LLCP) solutions, was predicted through the exact numerical calculation of Doi's diffusion equation without decoupling approximation by Larson [1990]. The existence of tumbling for TLCP is, however, controversial.

One assertion is associated with tumbling/wagging of directors as in LLCP. Another assertion is related to no tumbling but a technical problem involved in the measurement of first normal stress, that is, the method of how to set up the base line in the rheometer

[Langelaan and Gotsis, 1996]. According to Baek et al. [1994], the high viscosity caused by polymer-polymer dense packing and friction may be responsible for the disappearance of negative N_1 value. When a TLCP sample is loaded in nematic state for rheological measurement, normal stress N_1 is not completely relaxed and shows a residual normal stress, which is difficult to eliminate by heating the sample above the isotropization temperature because the TLCP may be degraded before reaching the isotropic state. When the unrelaxed state is set up as a base line, a negative N_1 may be observed [Kim and Han, 1993a, 1994; Langelaan and Gotsis, 1996]. A liquid crystalline polymer shows three regions of a viscosity curve, Region I, Region II and Region III in the shear rate [Asada et al., 1980]. In particular, it is known that the shear thinning in a low shear rate region (Region I) is ascribed to the presence of polydomain structure [Kim and Chung, 1997]. For the transient evolution of stress under shear flow, initial polydomain structure significantly affects the transient rheological behavior of TLCP.

The rheological properties of LCP are closely related to its structure formation on a micron scale as well as its pattern responding to the imposed flow condition, especially in the low shear rate region (Region I of Onogi-Asada's three region viscosity curve). However, the difficulty in rheology of LCP at a low shear rate arises for the qualitative as well as quantitative prediction of its dimensional inhomogeneity. Recently, a simple lattice model has been suggested, which is based on the heterogeneity in the director field [Bedford et al., 1991; Picken et al., 1992; Gervat et al., 1995]. Simulations of director dynamics were also carried out on the microstructural scale [Han and Rey, 1993; Ding and Yang, 1994]. Advantage of these models is that they are not necessarily of a delicate mathematical formulation in the complex and hierarchical structure of LCP orientation.

In this paper, the microstructural simulation of director evolution is based on the Frank free energy for the director distortion and on the Leslie-Ericksen hydrodynamic theory. It is carried out to inves-

*To whom correspondence should be addressed.

E-mail: chung@cais.kaist.ac.kr

tigate the texture evolution and the rheological change of a TLCP after the start-up of shear flow. Model parameters are of typical values of thermotropic liquid crystalline polymers and the moduli are of poly(ester-imide).

MICROSTRUCTURAL SIMULATION

1. Derivation of Constitutive Equation

In the Frank elasticity theory, the total energy for the spatial distortion of liquid crystal molecules can be given as

$$A_{el} = \frac{1}{2}K_1(\operatorname{div} \mathbf{n})^2 + \frac{1}{2}K_2(\mathbf{n} \cdot \operatorname{curl} \mathbf{n})^2 + \frac{1}{2}K_3(\mathbf{n} \times \operatorname{curl} \mathbf{n})^2 \quad (1)$$

where K_1 , K_2 and K_3 are the elastic constants for splay, twist and bend modes, respectively, and \mathbf{n} denotes a director vector at a local position. For TLCPs, the magnitude of elastic constants is in the following order: $K_1 \geq K_3 \gg K_2$ and the smallest twist mode (out-of-plane) is excluded automatically for a two-dimensional consideration. Typical values of K_1 and K_3 for TLCPs are 10^{-11} - 10^{-12} N [Lee and Meyer, 1988], which are about two orders larger than those for small molecule liquid crystals.

For a discrete two-dimensional lattice model without shear imposition [Picken et al., 1992], the approximate energy of the central cell is expressed as

$$\begin{aligned} (A_{el})_{center} &= \sum_k \frac{1}{2}(K_1 \sin^2 \vartheta_k + K_3 \cos^2 \vartheta_k) \sin^2(\phi_k - \theta) \\ &= \sum_k K(r \sin^2 \vartheta_k + (1-r) \cos^2 \vartheta_k) \sin^2(\phi_k - \theta) \end{aligned} \quad (2)$$

The angles θ and ϕ_k are defined in Fig. 1. ϑ_k is identified with ϕ_i for the right and left lattices and $\pi/2 - |\phi_i|$ for the upper and lower. Various energy functions for the discrete lattice model have been derived in the forms of $\sum \sin^2(\phi_k - \theta)$, $\sum (\phi_k - \theta)^2$ [Bedford et al., 1991] or $\sum (2 - 2\cos(\theta - \phi_k))$ [Kimura and Gray, 1993]. The energy function for the interaction between the adjacent cells takes

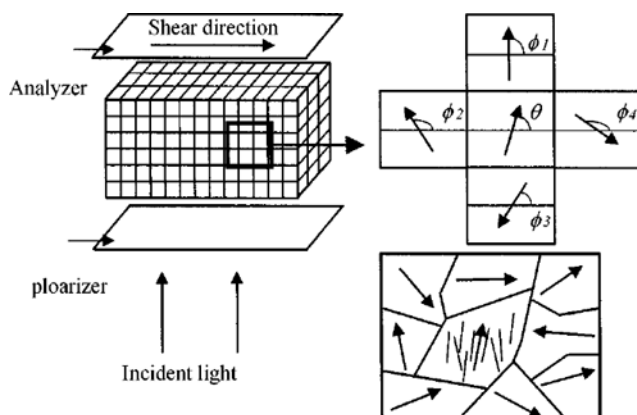


Fig. 1. Schematic diagram of array of lattice cells. Polydomain structure of liquid crystalline polymers through an optical microscope is modeled as directors in lattice cells. Definition of two-dimensional lattice for the microstructural simulations is shown and its dynamics is determined by the four adjacent director orientations and hydrodynamic torque exerted by shear flow. Directors in fact have no direction and therefore are in the range from -90° to 90°.

the form of $\sin^2(\phi_k - \theta)$ in this work. Although the energy function affects the final morphology [Assender and Windle, 1994], the above equations have a similarity in energy minimization procedure and slightly affect the morphological behavior under shear flow. The polydomain structure is observed by the simulation from the initial director distribution given arbitrarily. This texture formation corresponds to the real situation where the nematic texture is generated by cooling the isotropic melts of TLCPs below isotropization temperature. Spontaneous texture formation by energy minimization is thought to be successful in a sense that the order parameter value, $S = 0.5(3\langle \cos^2 \theta \rangle - 1)$, of about 0.3-0.4, coincides well with an experimental observation [Hongladarom and Burghardt, 1994].

In this work, director dynamics is obtained from the torque balance in a two-dimensional lattice model. The lattice model [Picken et al., 1992] is combined with the orientation change of directors [Semenov, 1993] with time. From the theory of hydrodynamics, the torque exerted on the central cell is approximated by

$$\frac{\theta(t + \Delta t) - \theta(t)}{\Delta t} = \frac{K'}{M} - \frac{\gamma}{2}(1 - \lambda \cos 2\theta) \quad (3)$$

where

$$\begin{aligned} M &= -\sum_i^4 (r \sin^2 \vartheta_i + (1-r) \cos^2 \vartheta_i) \sin(2(\phi_i - \theta)), \\ \vartheta_i &= \begin{cases} \phi_i & \text{for } i=2, 4 \\ \frac{\pi}{2} - |\phi_i| & \text{for } i=1, 3 \end{cases} \quad \lambda = \frac{1 + \alpha_2/\alpha_2}{1 - \alpha_2/\alpha_2} = -\frac{\gamma_2}{\gamma_1} \\ \gamma_1 &= \alpha_3 - \alpha_2, \quad \gamma_2 = \alpha_3 + \alpha_2, \quad K' = \frac{K}{a^2} \end{aligned} \quad (4)$$

Here, α_2 and α_3 are Leslie viscosities and a is the characteristic length of a lattice cell size. K is the average Frank elastic constant defined as $K_1 = 2Kr$ and $K_3 = 2K(1-r)$ where r is a sliding factor between bend and splay ($r=0.5$ is fixed in this simulation). Hence $r \sin^2 \vartheta_k + (1-r) \cos^2 \vartheta_k = 1$. The values of α_2 and α_3 are rarely reported for TLCPs, so the values used for the simulation are -415-170 of α_2 and -4 Pa·s of α_3 obtained for semiflexible thermotropic liquid crystalline polyester obtained from 4,4'-dioxy-2,2'-dimethyl azoxybenzenedodecanediyl [Donald and Windle, 1992]. The lattice size a is somewhat ambiguous. However, its possible minimum value is used, which takes the value of 10^{-7} m that corresponds to the contour length of aromatic polyester with degree of polymerization ca. 150. This means the minimum length scale cannot be smaller than the molecular level. The values of a , k and γ_i determine the rate of convergence in the simulation as discussed by Picken et al. [1992].

Because the lattice size a is 10^{-7} m, we have to take a 500×500 lattice to match the rheometer gap spacing of $50 \mu\text{m}$ (the domain size observed in experiment is order of $1\text{-}10 \mu\text{m}$). However, the comparison between the 50×50 and 500×500 lattice cases shows little difference in texture or stress after shear inception. This is due to the fact that the motion of directors does not differ for the two cases and the stress function $\langle \sin^2 \theta \cos^2 \theta \rangle$ is calculated on an average for all cells under shear flow. Thus, we have used the 50×50 lattice for all simulations. Perfect anchoring ($\theta=0$) boundary conditions are set for the upper and lower plates, and periodic boundary conditions are used at the right and left edges of the lattice. The

time interval of an iteration is set to 0.05 s.

STRESS EXPRESSION IN TERMS OF DIRECTOR ORIENTATION

At this time, we would like to consider the Leslie-Ericksen theory for the two-dimensional case under simple shear flow. This equation is usually adopted as a constitutive equation for the small molecule liquid crystal [Semenov, 1993]:

$$\sigma = \sigma_{yy} = \gamma \left\{ \frac{\alpha_3 + \alpha_4 + \alpha_5}{2} - \frac{\alpha_3^2}{\gamma_1} + \left(\alpha_1 + \frac{\gamma_2^2}{\gamma_1} \right) \sin^2 \theta \cos^2 \theta \right\} \quad (5)$$

where α_i 's are Leslie viscosities [de Gennes and Prost, 1992]. However, many molecular parameters (α_i 's) are used inconveniently and the relaxation of director orientation is not calculated like a small molecule liquid crystal in this equation. Thus, Eq. (5) is not thought to be adequate for the stress prediction of our TLCP. A direct application of Leslie-Ericksen theory to LCP rheology [Viola and Baird, 1986] has been shown to be insufficient for a quantitative prediction as well as for a qualitative one of transient behavior.

To obtain a proper stress expression using the director orientation resulting from the above simulation, we choose the theory of transverse isotropic liquid crystals developed by Larson and Mead [1989], which was derived for the theory of lyotropic LCPs. In this theory, the final stress expression in the monodomain is based on the director orientation only. We assume that the flow behavior of rodlike molecules in the lyotropic system has some similarity and is applicable to that in the thermotropic system. The stress expression is given on the basis of linear viscoelasticity:

$$\sigma_y = \int_{-\infty}^t \hat{G}_{ykl}(t-t') \gamma_{kl}(t') dt' \quad (6)$$

An anisotropic relaxational modulus $\hat{G}_{ykl}(t-t')$ has three distinct terms:

$$\begin{aligned} \hat{G}_{ykl}(t-t') = & 3ck_B T \left\{ \frac{(1-S)A}{3} (\delta_{yk}\delta_{jl} - n_x n_k \delta_{jl} - n_y n_k \delta_{jl}) \exp\left(-\frac{t-t'}{\lambda_1}\right) \right. \\ & + \frac{(1+2S)(1-S)(A-B)}{2} n_x n_y n_k n_l \exp\left(-\frac{t-t'}{\lambda_1}\right) \\ & \left. + \frac{A(1-S)}{2} n_x n_y n_k n_l \exp\left(-\frac{t-t'}{\lambda_1}\right) \right\} \end{aligned} \quad (7)$$

c is the number concentration of rods per unit volume, k_B is the Boltzmann constant, and T is absolute temperature. A and B are parameters depending on the scalar order parameter S and Maier-Saupe mean field potential U , respectively. There are two relaxation times λ_1 and λ_2 that can be expressed in terms of S , U , and rotational diffusivity (\bar{D}_r) of the rod molecules. Simplified to a two-dimensional case with $n_x = \cos \theta$ and $n_y = \sin \theta$, the shear component of relaxational moduli reduces to the form:

$$\hat{G}_{yyx}(t-t') + \hat{G}_{yyz}(t-t') = \sum_{u=1}^2 \Gamma_u^2 \sin^2 \theta \cos^2 \theta \exp\left(-\frac{t-t'}{\lambda_u}\right) \quad (7)$$

To apply the theory of lyotropes to thermotropes, the parameters Γ_u^2 in Eq. (7), are introduced and determined by the experiment, which includes all the parametric values (U , S , c , k_B , T , and \bar{D}_r) in the theory of Larson and Mead [1989]. The shear stress may be gen-

eralized and expressed as

$$\sigma_{yy} = \int_{-\infty}^t \sum_{i=2}^2 \Gamma_i^2 \langle \sin^2 \theta \cos^2 \theta \rangle \exp\left(-\frac{t-t'}{\lambda_i}\right) \gamma_{yy}(t') dt' \quad (8)$$

$\langle \cdot \rangle$ means the average over all the lattice cells. In the theoretical calculation, an expansion with multiple time constants has been frequently performed when the polydispersity effect is considered [Chow and Fuller, 1985; Larson and Mead, 1991]. In spite of the fact that Eq. (8) is derived from the theory of lyotropic LCPs, we adopt the equation as a constitutive equation because it is similar to the generalized Maxwell-type integral stress equation in which the constants Γ_i^2 will be determined from the experimental result. Similarly, first normal stress difference, N_1 is presented as follows:

$$N_1 = \sigma_{xx} - \sigma_{yy} = \int_{-\infty}^t \sum_{i=2}^2 \Gamma_i^2 \langle \cos^3 \theta \sin \theta - \sin^3 \theta \cos \theta \rangle \exp\left(-\frac{t-t'}{\lambda_i}\right) \gamma_{yy}(t') dt' \quad (9)$$

EXPERIMENTS

1. Materials

Methyl hydroquinone (MeHQ) was acetylated by means of acetic anhydride in boiling toluene with a catalytic amount of pyridine. The ω -amino acid and trimellitic anhydride were placed in dried dimethylformamide with toluene, and this mixture was refluxed for 4 hr in a flask. A mixture of N-(6-carboxyalkylene) trimellitic imides and hydroquinone diacetate with magnesium oxide was weighted in a round-bottomed cylindrical glass reactor equipped with a stainless steel stirrer. The reactants were condensed at 220–270 °C for about 7 hr under the nitrogen atmosphere, and then under vacuum for 1 hr at 270 °C. The poly(ester-imide) was synthesized and used for the test. Its schematic chemical structure is shown in Fig. 2.

2. Rheological Experiments

Polymer powder was dried in a vacuum oven at 80 °C for about 24 h to remove any residual solvent and moisture, and disk type samples (approximately 2 mm thickness and 25 mm diameter) were prepared and kept above the melting point of poly(ester-imide) at the pressure of 10 MPa for 5 min in a hot press. This poly(ester-imide) undergoes only two thermal transitions: (i) glass transition at ca. 68 °C and (ii) nematic-isotropic transition at ca. 179 °C.

An ARES with cone and plate fixture was used to measure (1) dynamic moduli (G' and G'') as function of the angular frequency, and (2) the shear stress growth and first normal stress difference growth after shear inception as a function of time for various shear rates. A cone angle of 0.1 rad was used; it had a diameter of 25 mm. All gap sizes were fixed at 50 μ m. All experiments were carried out under nitrogen atmosphere in order to preclude the oxidative

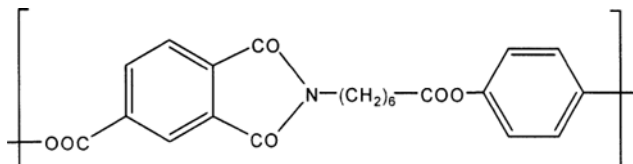


Fig. 2. Chemical structure of thermotropic liquid crystalline poly(ester-imide) used in this work.

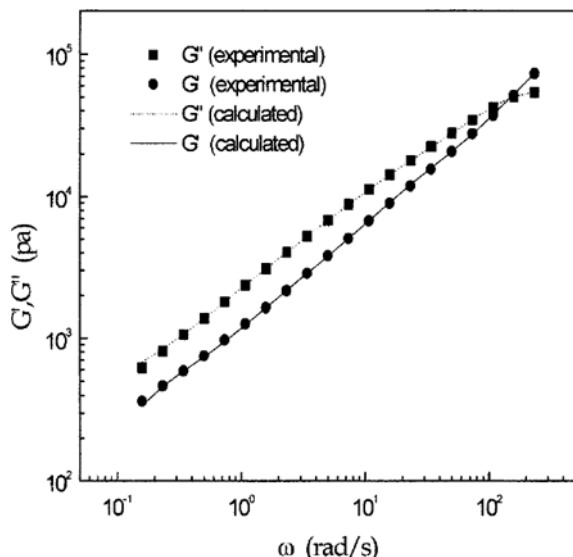


Fig. 3. Frequency sweep measurement of poly(ester-imide) with $\gamma=10\%$ at $140\text{ }^{\circ}\text{C}$. The symbols are measured values of G' and G'' . The solid line and dot line are calculated Maxwell elements from non-linear least square fitting.

degradation of samples. Temperature control was satisfactory within $\pm 0.1\text{ }^{\circ}\text{C}$. In a frequency sweep, the extent of strain amplitude was well within the linear viscoelastic range of materials investigated. After the sample was loaded at $190\text{ }^{\circ}\text{C}$ for 10 min, which is well above the isotropization temperature of poly(ester-imide), it was cooled down slowly to a predetermined temperature, and held for 10 min to equilibrate thermodynamically prior to measurements

RESULTS AND DISCUSSION

1. Frequency Sweep Measurement

From data in Fig. 3, we could obtain the Maxwell elements of relaxational moduli of our poly(ester-imide) by non-linear least square method [Bird et al., 1987; Kamath and Mackley, 1989]. The calculated moduli values are listed in Table 1. The symbols are experimental values; the solid line and dotted line are calculated values.

Thermal hysteresis of a viscoelastic property is found for various TLCPs, such as *p*-hydroxybenzoic acid (PHB)/poly(ethylene

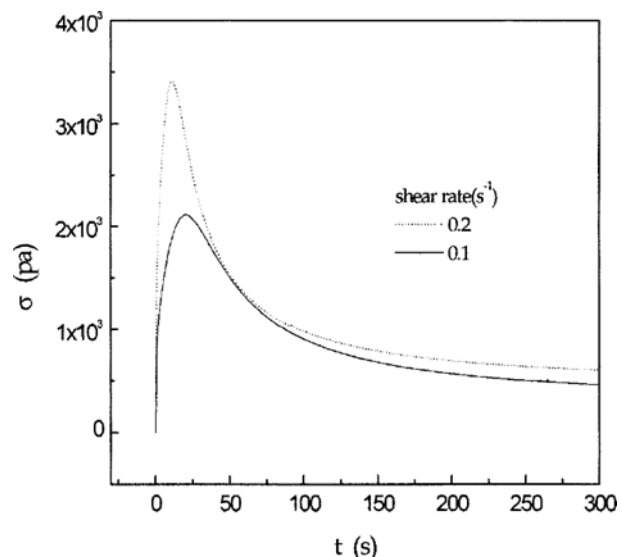


Fig. 4. Start-up shear stress measurement of poly(ester-imide) at $140\text{ }^{\circ}\text{C}$ with various shear rates.

terephthalate) (PET) and PHB/HNA copolyester [Done and Baird, 1990; Driscoll et al., 1994]. It may be due to the supercooling effect. In this work, poly(ester-imide) is thought to be very adequate for the test to examine the only effect of texture on the rheological properties of TLCPs, because the hysteresis and the formation of high temperature crystallization do not exist in this sample [Kim et al., 2000]. This unique rheological behavior has already been explained in terms of the monomeric sequence distribution compared with homopolymers by Kim et al. [1997a].

2. Start-up Shear Flow Measurement

Fig. 4 shows the stress growth after the startup of shear flow. It should be mentioned that a fresh sample was employed for each shear rate. Upon startup of shear flow, the shear stress, $\sigma(t, \gamma)$ goes through a maximum in a very short time. As the shear rate increases, the peak becomes higher and tends to shift towards a shorter time, although the extent of shift is seen to be rather small and the ratio of the maximum stress to the equilibrium stress $\sigma(t, \gamma)/\sigma_{\infty}(t, \gamma)$, is found to lie between 6.43 and 6.74. Such a large value of $\sigma(t, \gamma)/\sigma_{\infty}(t, \gamma)$ ratio is believed to be caused by the abrupt break-up of the polydomain structure at an early stage.

The evolution of the first normal stress difference $N_1(t, \gamma)$ with time is shown in Fig. 5 for the different shear rates. Upon startup of shear flow $N_1(t, \gamma)$ goes through a maximum, which becomes greater with increasing γ . At a high shear rate, $N_1(t, \gamma)$ goes down to a negative value at a very early stage of transient shear flow, but soon goes up to a positive value and reaches a positive of steady-state. The ratio of the maximum to the equilibrium value of first normal stress difference, $N_{1,\max}(t, \gamma)/N_1(\infty, \gamma)$ lies between 5.44 and 5.55, depending on the applied shear rate γ . Such large values of $N_{1,\max}(t, \gamma)/N_1(\infty, \gamma)$ ratio are believed to be characteristics of TLCPs in general and are attributable to the polydomains, which exist in the nematic state of a poly(ester-imide) before the application of sudden shear flow [Kim and Han, 1993].

In lytropes, the most reliable signature of tumbling is the presence of negative normal stresses in steady shear and stress oscillations in transient shear flows. It has been reported that the poly-

Table 1. Calculated pre-exponential relaxation moduli. Nine time constants in a range from and are selected and their corresponding Maxwell elements are obtained

i	Time constant λ_i (s)	Modulus Γ_i (Pa)
1	0.00112	8400.0
2	0.00316	8240.6
3	0.01212	8303.1
4	0.04642	1623.5
5	0.1778	550.38
6	0.6813	450.20
7	2.610	370.533
8	6.31	300.35
9	10.00	260.00

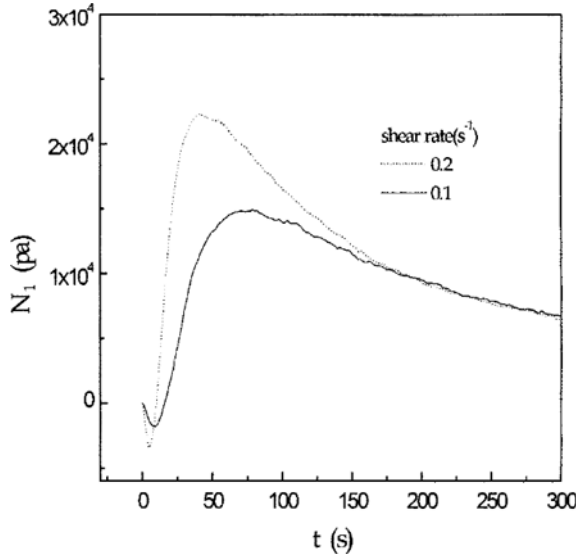


Fig. 5. Start-up first normal stress difference measurement of poly(ester-imide) at 140 °C with various shear rates.

mer-polymer dense packing and friction might obstruct the tumbling of rod-like molecules and be responsible for the disappearance of negative N_1 values in TLCPs [Baek et al., 1994]. Measurements in transient shear flows show no strong indication of the oscillatory responses of tumbling. Recently, using the same sort of material we found only positive values of N_1 in steady shear measurement.

A comparison of Fig. 4 with Fig. 5 shows that $N_1(t, \gamma)$ has the maximum at a larger value of time and takes a longer period to reach a steady state than $\sigma(t, \gamma)$.

3. Microstructural Simulation

As reported by many researchers, TLCP in the nematic state has a supra-molecular structure [Larson and Doi, 1991; Kim et al., 1994; Han and Rey, 1995; Langelaan and Gotsis, 1996]. Such a supra-molecular structure is often referred to as a polydomain, which may be regarded as aggregates consisting of many small-sized domains (monodomains). It can be postulated that when a sudden shear flow is applied to a TLCP in the nematic region, the domains will be broken up and the extent of destruction depends on the intensity of shear rate. When the flow is stopped, the broken domain texture will start to reorganize and coalesce to form polydomains, probably regaining the original domain texture if a sufficiently long time is allowed to elapse.

In this microstructural simulation, polydomain structure in a quiescent state is developed from the random configuration of initial director field. Textures appear [Fig. 6(a)] between the aligned aggregates of directors or domains, although every lattice cell is under an equivalent dynamics. Fig. 6 shows the director evolution after shear inception for shear rate 1 s^{-1} .

After shear inception, directors are in motion governed mainly by viscous torque and closely aligned to the flow direction with a Leslie angle $\Theta_L = \tan^{-1} \sqrt{\alpha_3/\alpha_2}$ [Fig. 6(b)-(d)]. In this work, the total energy of the system of LCP and relaxation moduli decrease as directors align in the shear direction, whereas the orientation parameter is increased. This result is contrary to the result of the solid model such as a calculation of an anisotropic aggregate model based on

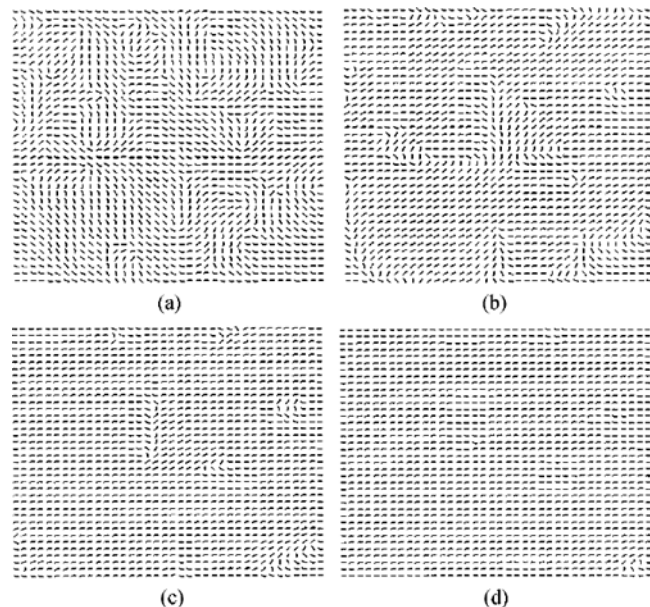


Fig. 6. Evolution of director field by means of the microstructural simulation.

(a) Textured director map through a Frank energy minimization. This director map is taken as an initial texture of start-up shear flow. (b) Textures after 1 s under a shear flow with $\gamma = 1 \text{ s}^{-1}$. (c) Texture after 2 s. (d) Texture after 25 s.

the lattice cell perpendicular to the shearing plane in that the shear modulus increases as the directors align in the shear or elongation direction [Gervat et al., 1995]. It has to be noted that the director orientation out of the shear plane produces no shear stress [Larson and Mead, 1989]. The fact that the post-sheared (aligned) TLCP shows lower moduli than the pre-sheared (unaligned) one has been known by the experimental results from the study about the effect of shear history on the small-oscillatory measurement [Driscoll et al., 1994]. This microstructural simulation explains a hydrodynamics of director in connection with polydomain texture in quiescent state and its break-up by shear imposition in a shearing plane.

It is noted that we take into account heterogeneity of TLCPs in this work. It is well known that there are inherent defects by the chain end. In addition, phase separation between high molecular weight LC phase and rather isotropic low molecular weight LC phase is known to cause a high density of defects in TLCP [Nakai et al., 1994]. The effects of these inherent defects are very important for the transient rheological properties. For a lattice simulation, the defects have been modeled by means of fixing some lattice orientation [Gervat et al., 1995].

Fig. 7 shows the calculated shear stress for a start-up shear flow from the simulation of Eq. (8). The values of Γ_i^0 in the equation are obtained by frequency sweep measurement. For the case of a single time constant, the Maxwell component Γ_i in Table 1 can be regarded as identical to the function of $\Gamma_i^0 \sin^2 \theta \cos^2 \theta$ for the initial director orientations. The total stress of TLCP can be calculated by using the pre-exponential part of moduli in Eq. (8) with the average director orientation at each time step. The ratio of the maximum to the equilibrium value of shear stress, $\sigma(t, \gamma)/\sigma_\infty(t, \gamma)$, lies between 1.2 and 2.95, depending on the applied shear rate γ . First normal stress difference is also calculated from Eq. (9) and is de-

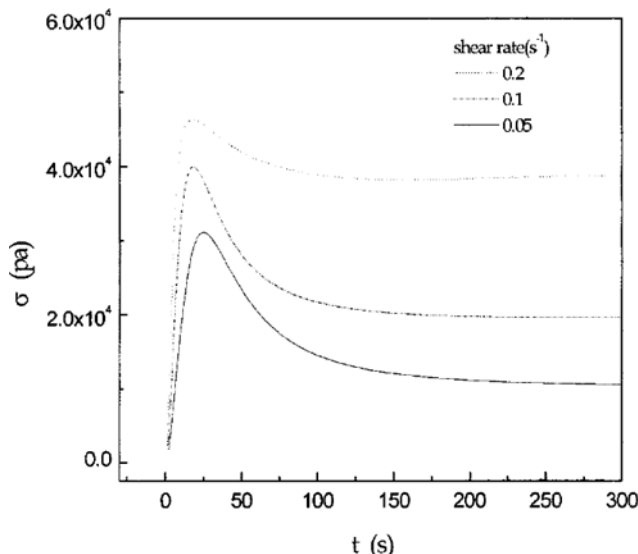


Fig. 7. Transient shear stress upon a start-up shear flow from the microstructural simulation.

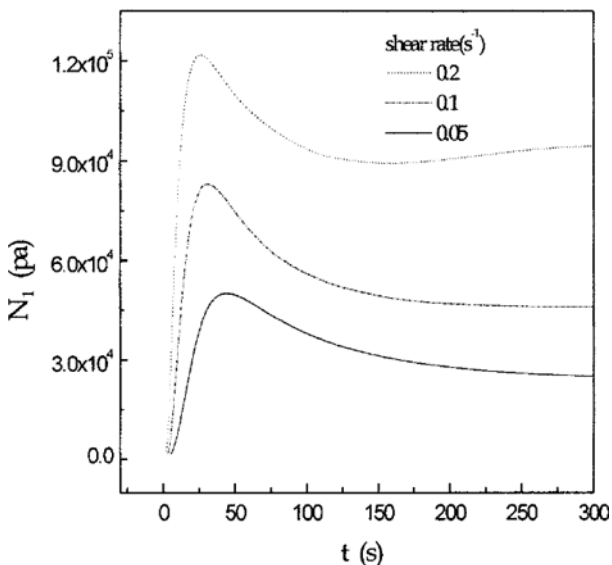


Fig. 8. Transient first normal stress difference upon a start-up shear flow from the microstructural simulation.

picted in Fig. 8. The ratio of the maximum to the equilibrium value of first normal stress difference, $N_{1,\max}(t, \gamma)/N_1(\infty, \gamma)$ lies between 1.36 and 1.95, depending on the applied shear rate γ . It also shows a single overshoot. In both of the calculated results, the faster appearance of maximum overshoot position with increasing the shear rate seems to be responsible for the faster decrease of pre-exponential moduli by the faster loosing of the polydomain structure.

Comparing experiment and simulation results (Fig. 4, 5, 7, 8), after startup of shear flow, both shear stress and first normal stress difference go through a maximum which is believed to be caused by the abrupt break-up of the polydomain structure at an early stage. As the shear rate increases, the peak becomes higher and tends to shift towards a shorter time.

In simulation and experiment results there are differences in the maximum magnitude of overshoot. This is attributed to a distortion

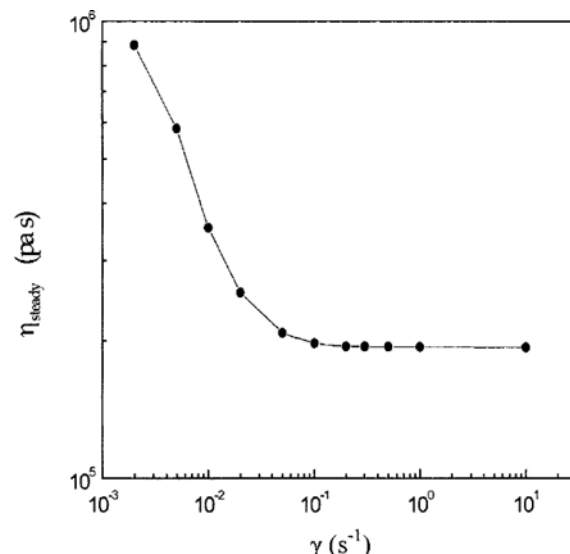


Fig. 9. Calculated steady shear viscosity from the microstructural simulation.

tional elasticity associated with the deformation of disclinations in the polydomain sample and defect density that is ascribed to fix some directors to represent a more real situation. The first normal stress difference in experiment shows a negative value, which may be caused by sample relaxed incompletely, at a very early stage of transient shear flow, but it does not in simulation.

Fig. 9 shows the calculated steady state shear viscosity as a function of shear rate. It shows shear thinning in the low shear rate range and a Newtonian plateau in the large shear rate region (Region I and Region II of Onogi-Asada's three-region viscosity curve). Such behavior is very important because it is a characteristic of TLCP, and this result is well consistent with experimental results [Chang and Han, 1997]. Shear thinning in the low shear rate region is believed to be caused by the abrupt break-up of the polydomain structure at an early stage.

CONCLUSIONS

The rheological behavior of a TLCP in the nematic phase is very unusual and shows quite different phenomena such as thermal hysteresis and high temperature crystallization. Thermal hysteresis is caused by the supercooling effect, and high temperature crystallization is caused by the existence of residual crystallites. Herein a new TLCP, poly(ester-imide), was synthesized to remove these unusual phenomena.

Model prediction by means of microstructural simulation shows a decrease in relaxation modulus of TLCP because the polydomain texture disappears as the directors align in the shear direction. Dynamic moduli obtained from the experiment are applied to the calculation of parameters in Eq. (8). In this manner the texture of TLCP is modeled from the proper parameters; for example, Frank elastic constants and the Maxwell type moduli obtained experimentally are used to predict $\sigma(t, \gamma)$ and $N_1(t, \gamma)$ for the start-up shear flow. The results of simulation are in agreement with the experimental results for TLCPs qualitatively. For a start-up shear flow the destruction of polydomain texture by flow and its resultant decrease

of shear moduli, which depend on the average orientation of directors, produce a large stress overshoot. Also, we could predict shear thinning in a low shear rate region (Region I), which is ascribed to the break-up of polydomain structure. It is possible to predict the flow behavior of a thermotropic polymer by using the lattice model and the rheological equations extending from the theories for lyotropic liquid crystalline polymers.

ACKNOWLEDGMENT

The authors thank Korea Science & Engineering Foundation for the partial financial support through the grants-in-aid (KOSEF 94-0300-04-01-3).

NOMENCLATURE

a	: a characteristic length of a lattice cell size
α_i	: Leslie viscosities
A_{el}	: the total energy for the spatial distortion of liquid crystal molecules
c	: a number concentration of rods per unit volume
G'	: storage modulus
G''	: loss modulus
K	: the average Frank elastic constant
K_1	: splay elastic constant
K_2	: bend elastic constant
k_B	: Boltzmann constant
M	: torque for the spatial distortion of liquid crystal molecules
n	: denotes a director vector at a local position
r	: sliding factor
S	: scalar order parameter
T	: absolute temperature
U	: Maier-Saupe mean field potential
ϕ	: angle of neighboring directors
σ	: shear stress
σ_∞	: steady shear stress
N_1	: first normal stress difference
$N_{1,max}$: maximum first normal stress difference for startup test
G_{yy}	: relaxational modulus
λ_i	: relaxation times
γ	: shear rate
Γ_u^o	: parameters which include the all parametric values (U , S , c , k_B , T , and \bar{D}_s) in the theory of Larson and Mead
θ	: angle of director
Θ_L	: Leslie angle

REFERENCES

Alderman, N. J. and Mackley, M. R., "Optical Textures Observed during the Shearing of Thermotropic Liquid-crystalline Polymers," *Faraday Disc. Chem. Soc.*, **79**, 149 (1985).

Asada, T., Muramatsu, H., Watanabe, R. and Onogi, S., "Rheo-optical Studies of Racemic Poly(γ -benzyl glutamate) Liquid Crystals," *Macromolecules*, **13**, 867 (1980).

Assender, H. E. and Windle, A. H., "Two-dimensional Lattice Model of Disclinations in Liquid Crystals: Choice of Energy Function,"

Macromolecules, **27**, 3239 (1994).

Baek, S. G., Magda, J. J., Larson, R. G. and Hudson, S. D., "Rheological Differences Among Liquid-Crystalline Polymers. II. Disappearance of Negative N_1 in Densely Packed Lyotropes and Thermotropes," *J. Rheol.*, **38**, 1473 (1994).

Bedford, S. E., Nicholson, T. M. and Windle, A. H., "A Supra-molecular Approach to the Modeling of Textures in Liquid Crystals," *Liq. Cryst.*, **10**, 63 (1991).

Bird, R. B., Armstrong, R. C. and Hassager, O., "Dynamics of Polymeric Liquids. Volume 1 Fluid Mechanics," 2nd Ed., John Wiley & Sons, New York (1987).

Chandrasekhar, S., "Liquid Crystals," 2nd Ed., Cambridge University Press, Cambridge (1992).

Chang, S. and Han, C. D., "A Thermotropic Main-Chain Random Copolyester Containing Flexible Spacers of Differing Lengths. 2. Rheological Behavior," *Macromolecules*, **30**, 1656 (1997).

Chow, A. W. and Fuller, G. G., "Rheological Response of Rodlike Chains Subjected to Transient Shear Flow. 1. Model Calculations on the Effects of Polydispersity," *Macromolecules*, **18**, 786 (1985).

Cochini, F., Nobile, M. R. and Acierno, D., "Letter: About Negative First Normal Stress Differences in a Thermotropic Liquid Crystalline Polymer," *J. Rheol.*, **36**, 1307 (1992).

Ding, J. and Yang, Y., "Brownian Dynamics Simulation of Rodlike Polymers under Shear Flow," *Rheol. Acta*, **33**, 405 (1994).

Doi, M., "Effect of Chain Flexibility on the Dynamics of Rodlike Polymers in the Entangled State," *J. Polym. Sci. Polym. Symp.*, **73**, 93 (1985).

Doi, M., "Molecular Dynamics and Rheological Properties of Concentrated Solutions of Rodlike Polymers in Isotropic and Liquid Crystalline Phases," *J. Polym. Sci. Polym. Phys. Ed.*, **19**, 229 (1981).

Donald, A. M. and Windle, A. H., "Liquid Crystalline Polymers," Cambridge University Press, Cambridge (1992).

Done, D. and Baird, D. G., "Solidification Behaviors and Recovery Kinetics of Liquid Crystalline Polymers," *Polym. Eng. Sci.*, **30**, 989 (1990).

Driscoll, P., Hayase, S. and Masuda, T., "Viscoelastic Properties of a 60 mol% para-Hydroxybenzoic Acid/40 mol% Poly(ethylene terephthalate) Liquid Crystalline Copolyester. II: Effect of Shear History," *Polym. Eng. Sci.*, **34**, 519 (1994).

De Gennes, P. G. and Prost, J., "The Physics of Liquid Crystals," 2nd Ed., Clarendon Press, Oxford (1992).

Gervat, L., Mackley, M. R., Nicholson, T. M. and Windle, A. H., "The Effect of Shear on Thermotropic Liquid Crystalline Polymers," *Phil. Trans. Roy. Soc. Lond.*, **A350**, 1 (1995).

Gleeson, J. T., Larson, R. G., Mead, D. W., Kiss, G. and Cladis, P. E., "Image Analysis of Shear-induced Textures in Liquid-crystalline Polymers," *Liq. Cryst.*, **11**, 341 (1992).

Guskey, S. M. and Winter, H. H., "Transient Shear Behaviors of a Thermotropic Liquid Crystalline Polymer in the Nematic State," *J. Rheol.*, **35**, 1191 (1991).

Han, C. D. and Chang, S., "Note: On the First Normal Stress Difference of the Thermotropic Copolyester 73/27 HBA/HNA," *J. Rheol.*, **38**, 241 (1994).

Han, W. H. and Rey, A. D., "Simulation and Validation of Temperature Effects on the Nematic rheology of Aligning and Nonaligning Liquid Crystals," *J. Rheol.*, **39**, 301 (1995).

Hanna, S. and Windle, A. H., "Geometric Limits to Order in Liquid

Crystalline Random Copolymers," *Polymer*, **29**, 207 (1988).

Hongladarom, K. and Burghardt, W. R., "Measurement of the Full Refractive Index Tensor in Sheared Liquid Crystalline Polymer Solutions," *Macromolecules*, **27**, 483 (1994).

Kamath, V. M. and Mackley, M. R., "The Determination of Polymer Relaxation Moduli and Memory Functions using Integral Transforms," *J. Non-Newtonian Fluid Mech.*, **32**, 119 (1989).

Kim, K. M. and Chung, I. J., "Structural Change of Polydomain in the Liquid Crystalline Polymers by Weak Shear Flow," *Korean J. Chem. Eng.*, **14** (1997).

Kim, K. M., Cho, H. and Chung, I. J., "Defect Density Evolution and Steady Rheological Behaviors of Liquid Crystalline Polymers," *J. Rheol.*, **38**, 1271 (1994).

Kim, S. O., Kim, T. K. and Chung, I. J., "Synthesis and Rheological Investigation on Phase Behaviors of Semiflexible Type Amorphous Liquid Crystalline Poly(ester-imide)s," *Polymer*, **41**, 4709 (2000).

Kim, S. S. and Han, C. D., "Effect of Shear History on the Steady Shear Flow Behavior of a Thermotropic Liquid-crystalline Polymer," *J. Polym. Sci. Part B: Polym. Phys.*, **32**, 371 (1994).

Kim, S. S. and Han, C. D., "Effect of Thermal History on the Rheological Behavior of a Thermotropic Liquid-crystalline Polymer," *Macromolecules*, **26**, 3176 (1993a).

Kim, S. S. and Han, C. D., "Transient Rheological Behavior of a Thermotropic Liquid Crystalline Polymer. I. The Start-up of Shear Flow," *J. Rheol.*, **37**, 847 (1993b).

Kim, T. K., Kim, K. M. and Chung, I. J., "Effects of Monomeric Sequence Distribution on Physical Properties of Thermotropic Liquid Crystalline Copoly(ester-imide)s," *Polym. J.*, **29**, 85 (1997a).

Kim, T. K., Kim, S. O. and Chung, I. J., "Synthesis and Characterization of Thermotropic Liquid Crystalline Copoly(ester-imide)s," *Polym. Adv. Technol.*, **8**, 305 (1997).

Kimura, T. and Gray, D. G., "Annealing Method for Modeling Liquid Crystal Textures," *Macromolecules*, **26**, 3455 (1993).

Kiss, G. and Porter, R. S., "Rheology of Concentrated Solutions of Poly(γ -benzyl-glutamate)," *J. Polym. Sci. Polym. Symp.*, **65**, 193 (1978).

Kleman, M., Liebert, L. and Strezelecki, L., "Preliminary Observations of Defects in a Polymeric Nematic Phase," *Polymer*, **24**, 295 (1983).

Langelaan, H. C. and Gotsis, A. D., "The Relaxation of Shear and Normal Stresses of Nematic Liquid Crystalline Polymers in Squeezing and Shear Flows," *J. Rheol.*, **40**, 107 (1996).

Larson, R. G. "Arrested Tumbling in Shearing Flows of Liquid Crystal Polymers," *Macromolecules*, **23**, 3983 (1990).

Larson, R. G. and Doi, M., "Mesoscopic Domain Theory for Textured Liquid Crystalline Polymers," *J. Rheol.*, **35**, 539 (1991).

Larson, R. G. and Mead, D. W., "Linear Viscoelasticity of Nematic Liquid Crystalline Polymers," *J. Rheol.*, **33**, 185 (1989).

Larson, R. G. and Mead, D. W., "Toward A Quantitative Theory of the Rheology of Concentrated Solutions of Stiff Polymers," *J. Polym. Sci. Polym. Phys. Ed.*, **29**, 1271 (1991).

Lee, S. D. and Meyer, R. B., "Crossover Behavior of the Elastic Coefficients and Viscosities of a Polymeric Nematic Liquid Crystal," *Phys. Rev. Lett.*, **61**, 2217 (1988).

Lin, Y. G. and Winter, H. H., "Formation of a High Melting Crystals in a Thermotropic Aromatic Copolyester," *Macromolecules*, **21**, 2439 (1989).

Marrucci, G. and Grizzuti, N., "The Effect of Polydispersity on Rotational Diffusivity and Shear Viscosity of Rodlike Polymers in Concentrated Solutions," *J. Polym. Sci. Polym. Lett. Ed.*, **21**, 83 (1983).

Nakai, A., Wang, W., Hashimoto, T., Blumstein, A. and Maeda, Y., "Phase Separation Process and Self-organization of Textures in the Biphase Region of Thermotropic Liquid Crystalline Poly(4,4-dioxy-2,2-dimethylazoxybenzene-dodecanedioyl). 1. A Study on the Athermal Conditions," *Macromolecules*, **27**, 6963 (1994).

Picken, S. J., Moldenaers, P., Berghmans, S. and Mewis, J., "Experimental and Theoretical Analysis of Band Formation in Polymeric Liquid Crystals Upon Cessation of Flow," *Macromolecules*, **25**, 4759 (1992).

Semenov, A. N., "Domain Formation in Liquid Crystals Under Oscillating Shear Flow," *J. Rheol.*, **37**, 911 (1993).

Viola, G. G. and Baird, D. G., "Studies on the Transient Shear Flow Behavior of Liquid Crystalline Polymers," *J. Rheol.*, **30**, 601 (1986).

Winter, H. H. and Wedler, W., "Note: About Measuring the First Normal Stress Difference in Shear Flow of a Thermotropic Copolyester," *J. Rheol.*, **37**, 409 (1993).

Wissbrun, K. F., "Observations on the Melt Rheology of Thermotropic Aromatic Polyesters," *Brit. Polym. J.*, **12**, 163 (1980).